THE JOURNAL OF BIOLOGICAL CHEMISTRY VOL. 286, NO. 12, pp. 10834–10846, March 25, 2011

The Syntaxin 4 N Terminus Regulates Its Basolateral Targeting by Munc18c-dependent and -independent Mechanisms*[S]

Received for publication, September 22, 2010, and in revised form, January 14, 2011 Published, JBC Papers in Press, January 28, 2011, DOI 10.1074/jbc.M110.186668

Jacqueline Torres, Holly M. Funk[1], Mirjam M. P. Zegers, and Martin B. A. ter Beest[2]

From the Department of Surgery, The University of Chicago, Chicago, Illinois 60637

To generate and maintain epithelial cell polarity, specific sorting of proteins into vesicles destined for the apical and basolateral domain is required. Syntaxin 3 and 4 are apical and basolateral SNARE proteins important for the specificity of vesicle fusion at the apical and basolateral plasma membrane domains, respectively, but how these proteins are specifically targeted to these domains themselves is unclear. Munc18/SM proteins are potential regulators of this process. Like syntaxins, they are crucial for exocytosis and vesicle fusion. However, how munc18c and syntaxin 4 regulate the function of each other is unclear. Here, we investigated the requirement of syntaxin 4 in the delivery of basolateral membrane and secretory proteins, the basolateral targeting of syntaxin 4, and the role of munc18c in this targeting. Depletion of syntaxin 4 resulted in significant reduction of basolateral targeting, suggesting no compensation by other syntaxin forms. Mutational analysis identified amino acids Leu-25 and to a lesser extent Val-26 as essential for correct localization of syntaxin 4. Recently, it was shown that the N-terminal peptide of syntaxin 4 is involved in binding to munc18c. A mutation in this region that affects munc18c binding shows that munc18c binding is required for stabilization of syntaxin 4 at the plasma membrane but not for its correct targeting. We conclude that the N terminus serves two functions in membrane targeting. First, it harbors the sorting motif, which targets syntaxin 4 basolaterally in a munc18c-independent manner and second, it allows for munc18c binding, which stabilizes the protein in a munc18c-dependent manner.

To generate and maintain membrane polarization in epithelial cells it is essential that proteins are correctly sorted to their target membrane. Different protein machineries are involved in directing this polarized trafficking to the apical and basolateral membranes (1, 2). The final step in membrane targeting is fusion of the transport vesicle to the plasma membrane, which is mediated by members of the SNARE protein family. It has now been well established that epithelial cells express different forms of the SNARE protein syntaxin (3, 4). Syntaxin 3 and 4 specifically localize at the apical and basolateral surfaces, respectively. This polarized distribution is thought to provide a final level of specificity during membrane targeting, allowing for specific recognition of either the apical or basolateral membranes. Indeed, several studies have shown that syntaxin 3 and 4 are involved in, respectively, apical and basolateral membrane targeting in MDCK[3] cells (5, 6).

Although these studies showed that syntaxins play a crucial role in polarized membrane targeting, the exact requirements for the different syntaxin forms in the specificity of membrane delivery in epithelial cells is still unclear. We previously showed that redirecting syntaxin 3 to the basolateral membrane resulted in mistargeting of apical proteins (7). Also, mutations that cause basolateral missorting of syntaxin 3 interfered with the formation of tight junctions (8). This suggests that at least syntaxin 3 contributes to the specificity of membrane fusion. There are many differences in the regulation of apical and basolateral transport and whether syntaxin 4 plays an identical role in the specificity of basolateral membrane fusion is currently unknown. Furthermore, it is not known how syntaxin 4 itself is specifically targeted to the basolateral membrane. Syntaxin 4 function has been extensively studied in Glut4 transport and insulin secretion. In these studies, its interaction with the SNARE accessory protein munc18c was shown to be important for its function (9–11).

Munc18c is a member of the S/M (sec1/munc18) protein family, a group of proteins that are essential for exocytosis (12–14). They strongly bind to syntaxins and the different S/M proteins show a high binding specificity for different syntaxins. Recently it has been recognized that they are likely to play an active role in membrane fusion (15, 16). The shared function and strong and specific binding of S/M proteins to syntaxin suggest that they are crucial regulators of syntaxin function, but the exact function of this family of proteins is still unclear. S/M proteins may either stimulate or inhibit the function of syntaxins, which may depend on the way they interact with syntaxins.

In this study we have investigated the requirements for syntaxin 4 and munc18c in basolateral vesicle fusion and cell polarization. We show that syntaxin 4 is essential for basolateral protein delivery but not for the initial establishment of membrane polarity. We identified residues that are required for

* This work was supported by a grant from the American Cancer Society, Ohio Division (to M. B. A. t. B.) and by National Institutes of Health Grant GM076363 (to M. M. P. Z.).

[S] The on-line version of this article (available at http://www.jbc.org) contains supplemental Figs. S1–S6.

[1] Present address: Dept. of Cancer and Cell Biology, University of Cincinnati, Cincinnati, OH 45267.

[2] To whom correspondence should be addressed: 5841 South Maryland Ave., AB532/MC5032, Chicago, IL 60637. Tel.: 773-834-3272; Fax: 773-834-4546; E-mail: mterbe@surgery.bsd.uchicago.

[3] The abbreviations used are: MDCK, Madin-Darby canine kidney; VSV-G, vesicular stomatitis virus glycoprotein G; syn4KD, syntaxin 4 knockdown; dox, doxycycline.

basolateral sorting of syntaxin 4 in MDCK cells. Mutation of these residues resulted in non-polarized targeting of syntaxin 4, but expression of these mutants in syntaxin 4-depleted cells did not result in missorting of other basolateral proteins. We also focused on the role of the munc18c in syntaxin 4 sorting and function. Mutations in syntaxin 4 that abolish munc18c binding or munc18c knockdown did not have any effect on the localization of syntaxin 4. However, introducing mutations in syntaxin 4 that affect both the trafficking and munc18c binding results in intracellular localization of syntaxin 4. We, furthermore, show that a syntaxin 4 mutant that cannot bind munc18c rescues basolateral protein targeting in syntaxin 4-depleted cells as efficient as syntaxin 4. Our data suggests that in MDCK cells munc18c is not directly involved in the polarized localization of syntaxin 4 but is necessary for stabilizing syntaxin 4 at the plasma membrane. Finally, our data indicate that the transport and roles of syntaxin 4 at the basolateral domain are distinctly different from those of syntaxin 3 at the apical surface.

EXPERIMENTAL PROCEDURES

Antibodies—The following antibodies were used. Rabbit anti-syntaxin 4 (Calbiochem, San Diego, CA), rabbit anti-syntaxin 3 (7), rabbit anti-GFP (Rockland, Gilbertville, PA), mouse anti-GFP (Roche Applied Science), rabbit anti-FLAG, mouse anti-FLAG M2, mouse anti-Na,K-ATPase β1 chain, rabbit anti-SNAP23, mouse anti-E-cadherin DECMA (Sigma), mouse anti-E-cadherin, mouse anti-β1-integrin, mouse syntaxin 4 (BD Biosciences), rat anti-β1-integrin clone AIIB2 (17), rat anti-ZO-1 clone R40.76 (18), rabbit anti-claudin 2 (Invitrogen), mouse anti-p58 clone 6.23.3 (19), mouse anti-gp135 clone 3F21D8 (20), mouse anti-LAMP2 clone AC17 (21), rabbit anti-occludin (Zymed Laboratories Inc.), goat anti-Scribble, rabbit anti-β-catenin (Santa Cruz Biotechnology), and rabbit anti-syntaxin 2 and mouse anti-sec6 (StressGen Biotechnologies, Victoria, Canada). The rabbit anti-canine munc18c was raised to a C-terminal peptide of canine munc18c as immunogen (Sigma). Alexa secondary antibodies were obtained from Invitrogen, Li-Cor 800 secondary antibodies were from Li-Cor Biosciences, Lincoln, NE, and HRP-conjugated antibodies from Jackson ImmunoResearch Laboratories, West Grove, PA.

shRNA, cDNA Constructs, and Mutagenesis—To generate shRNA constructs, oligos specific for syntaxin 4 and munc18c knockdown were designed using standard procedures. To reduce off-target responses, the sequences were analyzed for possible homology with other sequences searching the dog genome project using the NCBI Blast Server. Oligos designed to canine syntaxin 4 (syn4KD2, 5′-CCGGATTGAGAAGAACATC-3′, and syn4KD3, 5′GCGAGGTGTTTGTATCCAA-3′) or munc18c specific sequences (munc18cKD1, 5′-ATCCTGGAGTAAGATATAA-3′, and munc18cKD2, 5′-GGATAGGTCTACAGAAGAA-3′) from Invitrogen were annealed and ligated into pTER (22) (kindly provided by Dr. J. Chernoff). For making stable knockdown cell lines, the H1-tet promoter and the targeting sequences were subcloned into pCDNA6-V5/His blasticidin in which the cytomegalovirus promotor was removed.

To make C-terminal-tagged syntaxin 4, the stop codon was removed and a SalI restriction site was introduced by PCR and inserted into pEGFP-N1 or pCDNA6 myc/His B. Mutations were made with the Stratagene QuikChange mutagenesis kit (Stratagene, La Jolla, CA). All sequences were verified by sequencing at the University of Chicago Cancer Research Center DNA sequencing facility.

Cell Culture, Transfection, and Nucleofection—MDCK II, T23, and Munc18c-FLAG expressing cells have been described previously (7). They were maintained in minimal essential medium with Earle's salts (Cellgro) supplemented with penicillin/streptomycin, 2 mM L-glutamine, and 10% FBS. LLC-PK1 cells were maintained in minimal essential medium-α with penicillin/streptomycin, 2 mM L-glutamine, and 10% FBS. Fisher rat thyroid cells were grown in Coon's modified Ham's F-12 medium supplemented with glutamine, penicillin/streptomycin, and 10% FBS. For each experiment, cells were grown on 12- or 24-mm 0.4-μm polycarbonate Transwells filters (Costar) for 4–5 days. In some cases cells were grown for 8 days. Medium was changed every other day and the day before an experiment. Transient nucleofections for gene expression were done using the Amaxa nucleofector using the L-buffer and program L-005 according to the manufacturer's protocol with modifications (23). Cells were plated on 12-mm Transwells and analyzed 2 and 3 days after nucleofection. To determine the efficacy of the shRNA constructs, cells were nucleofected using Amaxa T-buffer and program T-023 and cells were analyzed 2, 3, and 4 days after nucleofection. Stable shRNA-mediated knockdown cell lines were made using the calcium phosphate procedure as previously described (7). Cells were selected with 12.5 μg/ml of blasticidin and screened for knockdown by Western blot analysis. Cell lines were maintained in 10 μg/ml of blasticidin. Prior to experiments, the cells were washed and maintained in normal minimal essential medium with penicillin/streptomycin and 10% FBS. Stable inducible expression cell lines were made as described previously using the T23 MDCK tet-off cell line (7).

Determination of Integrity of the Monolayer—The integrity of the epithelial monolayer of cells grown for 5 days on Transwells was determined as described (24). Cells were washed 3 times with PBS with calcium and magnesium (PBS^+) PBS^+, 0.5 ml of PBS^+ with 100 μg/ml of FITC-inulin was added to the apical compartment, whereas 0.5 ml of PBS^{2+} was added to the basolateral compartment. After incubation for 30 min at 37 °C, 200-μl samples were taken from the apical and basolateral compartments. Fluorescence was determined using a fluorescent plate reader. Cells treated with 2 mM EDTA were used as a control for maximal leakage. The results are the mean ± S.D. of three independent experiments.

Confocal Fluorescence Microscopy—Immunostaining was done as described previously (7). To stain endogenous syntaxin 4, cells were fixed with methanol at −20 °C for 10 min. Alexa 488 or Alexa 555 were used as secondary antibodies. Alexa 555 phalloidin (Invitrogen) was used to stain filamentous actin. Cells were mounted in Fluorsave supplemented with DAPI. Samples were visualized using a Zeiss LSM 510 with an Axiovert 200M microscope and a C-Apochromat ×63/1.2W Corr lens. Images were analyzed using ImageJ for Mac version 1.40g. Composite images with scale bars were made using Adobe Photoshop CS version 9.0 and placed into Illustrator CS2 version 12.0.0.

For live cell imaging, cells were grown on the bottom of a 6.5-mm Transwell for 5 days as described (25). Cells were infected with adenovirus for VSV-G-EGFP-tsO45 as described (7). We found increased expression levels of VSV-G-EGFP-tsO45 in syn4KD cells, which is likely the result of more exposed adenovirus receptor. We adjusted the amount of virus to obtain similar levels of VSV-G-EGFP-tsO45 (60 infectious units/cell for control cells and 15 infectious units/cell for syn4KD3 cells). Titers were determined using an adenovirus immunoassay kit (Cell Biolabs, San Diego, CA). Infected cells were incubated overnight at 39.5 °C to allow accumulation of VSV-G-EGFP into the ER. Next, the cells were washed in Hanks' balanced salt solution and incubated for 2 h at 19.5 °C to allow accumulation of VSV-G-EGFP in the Golgi. After this incubation, cells were transferred into minimal essential medium without phenol red containing penicillin/streptomycin, 10% FBS, 20 mM Hepes, pH 7.5, and 10 μg/ml of cycloheximide and placed on a 35-mm MatTek dish with number 1.5 coverglass (MatTek, Ashland, MA) containing the same medium preincubated at 32 °C in a Pecon XL3-LSM temperature and CO_2 controlled chamber. The lag time between installing the Transwell and imaging was 2 min. In a typical experiment, *Z*-stacks with 6 images were obtained with a delay of 30 s for 30–45 min with the Zeiss autofocus macro. Horizontal image drift was corrected using the Stackreg plugin for ImageJ (26). Fluorescence in intracellular areas or areas that overlap the plasma membrane were quantified using ImageJ and represented as a relative increase of fluorescence. This was done for 12 cells for each condition and the average with standard deviations were calculated.

Co-immunoprecipitation Studies—For co-immunoprecipitation studies, cells were grown on 24-mm Transwells for 5 days. Cells were washed 2 times with PBS^+, cut out, and lysed in 800 μl of lysis buffer (25 mM Hepes-NaOH, pH 7.4, 150 mM NaCl, 5 mM EDTA, 1% Triton X-100, 1 mM NaF, 1 mM sodium vanadate and protease inhibitors). Lysates were precleared with Sepharose CL-4B beads (GE Healthcare) and equivalent amounts of protein were taken for the immunoprecipitation. In most cases 1 μg of antibody or 5 μl of antiserum was added to the lysates and incubated at 4 °C for 30 min. Sepharose-Protein A or G was added and incubated for 2 h at 4 °C while rotating. The beads were washed 4 times with lysis buffer by centrifugation. Proteins were eluted from the beads by boiling for 5 min in sample buffer with 100 mM DTT and the samples were, together with the lysates (5% of total), analyzed by SDS-polyacrylamide gel electrophoresis and Western blotting. For quantitative Western analysis, the PVDF (Immobilon, Millipore) membranes were first blocked with Odyssey Blocking buffer, probed with primary antibodies followed by Li-Cor 800 dye-conjugated antibodies (Li-Cor Biosciences) or Alexa 680-conjugated antibodies in Odyssey Blocking Buffer. Membranes were scanned using an Odyssey Infrared scanner. Protein bands were quantified with Odyssey 2.0 software. In some cases the standard enhanced chemiluminescence technique (ECL) was used to detect proteins. In that case 5% milk powder in PBS/Tween was used as blocking buffer and for incubation with primary and secondary antibodies.

Biotinylation Experiments—Biotinylation experiments for E-cadherin of β1-integrin were done as described (7). Briefly, control and syntaxin 4 knockdown cells were grown for 5 days on Transwells and washed in 3× PBS^+. Cells were incubated 2× 15 min with PBS^+ containing 500 μg/ml of EZ-Link Sulfo-NHS-Biotin (Pierce) at the apical or basolateral side of the Transwell. Reactive biotin was quenched by washing the cells 5 times with 50 mM NH_4Cl in PBS^+. After washing, cells were lysed in RIPA buffer (20 mM Tris-HCl, pH 7.5, 150 mM NaCl, 0.1% SDS, 1% deoxycholate, 1% Triton X-100, 5 mM EDTA and protease inhibitors) and immunoprecipitated as described above. Samples were analyzed by SDS-polyacrylamide gel electrophoresis, transferred to PVDF, and the blots were probed with IRDye 800CW-Streptavidin (LI-Cor, Lincoln, NE). Blots were stripped and reprobed for E-cadherin or β1-integrin.

To analyze p58, cells were biotinylated with EZ-Link Sulfo-NHS-SS-Biotin and biotinylated proteins were pulled down using Neutravidin beads (Pierce). Proteins were eluted from the beads by incubating the beads at 60 °C for 10 min in sample buffer with 100 mM DTT. Samples were analyzed by Western blot and probed with an antibody specific to Na,K-ATPase β1 chain.

For determining the polarity of the different syntaxin 4 constructs, we used different cell lines that express syntaxin 4-WT-EGFP and mutants. Using immunofluorescence, we determined conditions that result in similar expression levels at a cellular level. However, as not every cell shows expression, total expression levels are not the same for each cell line. The different cell lines were biotinylated as described above and the amount of pulled down biotinylated syntaxin 4-EGFP was determined by probing the blots with syntaxin 4 antibody. To determine significance, a paired Student's *t* test was performed on all quantitative experiments described above.

RESULTS

Knockdown of Syntaxin 4 Affects Basolateral Polarity—To study the function of syntaxin 4 in epithelial cells, we developed MDCK cell lines that were depleted in syntaxin 4. We designed and tested three shRNA constructs directed to three different sequences in the canine syntaxin 4. Transient expression of two of these constructs (syn4KD2 and syn4KD3) reduced syntaxin 4 levels by 80–90% and were used to make cell lines depleted in syntaxin 4 (Fig. 1*A*). These hairpins did not affect expression levels of other syntaxins but decreased munc18c expression levels (see supplemental Fig. S1*A*). This is not the result of non-specific silencing, but rather reflects the close interdependence of syntaxin 4 and munc18c expression (27, 28). For our next studies we used cell lines syn4KD2 c20 and syn4KD3 c9. As a control we made cell lines transfected with hairpins directed to GFP (GFPKD) or Luciferase (LucKD) (29). Both cell lines were used as controls in all the described experiments.

The syntaxin 4 knockdown (syn4KD) cell lines grew normal on plastic tissue culture plates and did not have an aberrant phenotype. Cell death and proliferation rates were also similar for syn4KD and control cells (not shown). However, when grown on permeable membranes, the cells showed an aberrant morphology with extended bulging apical domains, which

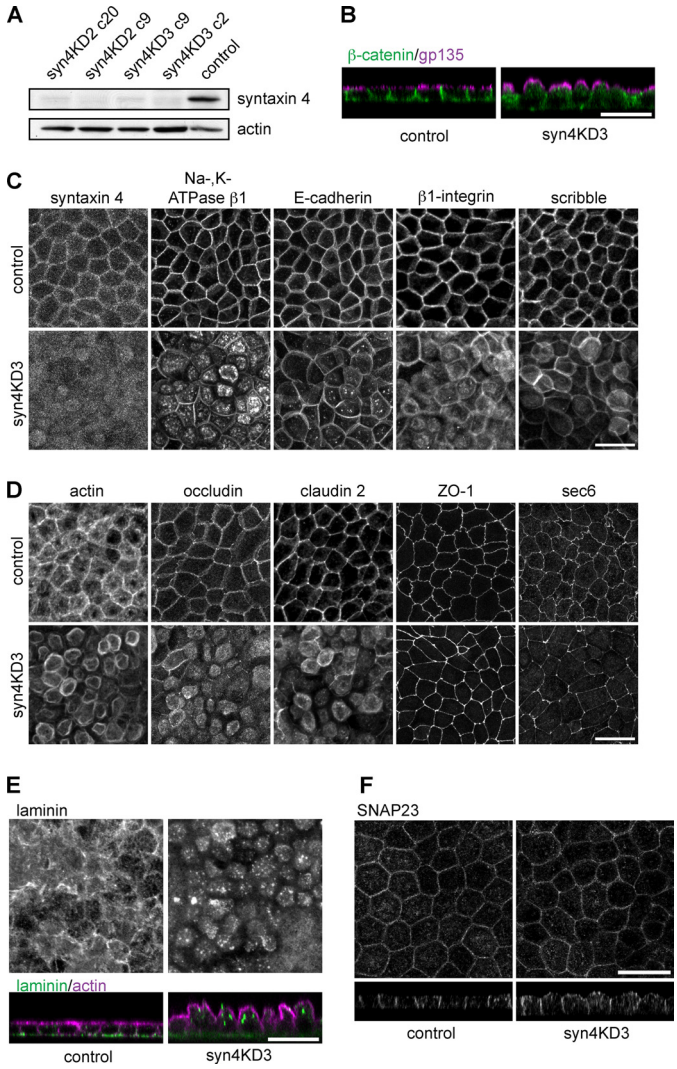

FIGURE 1. **Knockdown of syntaxin 4 results in inhibition of basolateral trafficking.** *A,* Western blot analysis of syntaxin 4 expression levels in cells expressing two different hairpins to syntaxin 4 (KD2 and KD3). Two clones for each hairpin are shown. A cell line expressing a hairpin to GFP (GFPKD) was used as a control cell line. Actin is the loading control. *B–F,* MDCK cell line depleted in syntaxin 4 (*syn4KD3*) and a control cell line (GFPKD) were grown for 5 days on filter, fixed, and stained. *B,* gp135/podocalyxin (*magenta*) and β-catenin (*green*) (*z*-scan). *C,* cells stained for several different basolateral proteins (syntaxin 4, Na,K-ATPase β1, E-cadherin, β1-integrin, and Scribble). *D,* cells stained for tight junction proteins (occludin, ZO-1, claudin 2, and sec6). Staining for actin is also shown. Images represent projections of several *x-y* scans. Representative single *x-y* scans are shown under supplemental Fig. S1*B*. *E,* cells stained for laminin (*top*, projections of *x-y* scans) and laminin (*green*) and actin (*magenta*) (*bottom*, *z*-scans). *F,* cells stained for SNAP23. *Scale bars,* 20 μm.

stained positive for the apical protein gp135/podocalyxin (Fig. 1*B*).

The basolateral staining for β-catenin was reduced in syn4KD cells (Fig. 1*B*), indicating that basolateral protein delivery is affected. To investigate this further, we stained for several other basolateral proteins (Fig. 1*C*, images show projections of *Z*-scans supplemental Fig. 1*B* shows single *x-y* scans of these images). As expected, syntaxin 4 expression was strongly reduced as the syn4KD cells are characterized by the absence of the typical honeycombed staining of syntaxin 4 (Fig. 1*C*, residual fluorescence is most likely background staining). Antibodies to the basolateral proteins E-cadherin, β1-integrin, and in particular p58 (which recognizes β1-chain of the Na,K-ATPase (30)) showed substantial increase of intracellular staining (Fig. 1*C*). Most of this staining was diffuse but we also observed localization in intracellular compartments for all antibodies. Similar results were obtained for knockdown cells lines made with different hairpins (supplemental Fig. 1*C*). Interestingly, the basolateral localization of E-cadherin was less sensitive to syntaxin 4 ablation as compared with other basolateral proteins. However, when cells were grown for longer periods (7–9 days on filter), a more significant reduction of basolateral E-cadherin staining was observed (supplemental Fig. S1*D*). We also analyzed the localization of Scribble, a polarity protein that directs the formation of the basolateral domain (31) and is localized basolateral (32). Scribble localized mostly basolateral in syn4KD cells, although some diffuse intracellular Scribble was observed (see also supplemental Fig. S1*B*).

We next examined the localization of several tight junction proteins and the exocyst protein sec6 (Fig. 1*D*). Interestingly, syntaxin 4 depletion affected some, but not all tight junction proteins. Staining for ZO-1 and the exocyst protein sec6 were not affected by syntaxin 4 knockdown. However, occludin and claudin 2 showed aberrant localization in the syntaxin 4KD cells, as some tight junction proteins are not correctly localized we would expect significant effects on the integrity of the epithelial layer. However, determining the epithelial integrity using leakage of FITC-inulin from the apical compartment showed no significant difference between control and syn4KD3 cells (supplemental Fig. 1*E*). This suggests that syn4KD cells partly maintain their tight junctions and form a monolayer impermeable for small molecules.

We next tested if secretion of basolateral proteins was affected in syn4KD cells. For this, we stained cells with an antibody for the secreted protein laminin-111 (which recognizes laminin β1 and γ1 chains) and found less deposited laminin and increased intracellular staining (Fig. 1*E*). This indicates that syntaxin 4 is also required for basolateral secretion. Finally, we found that localization of endogenous SNAP23, another plasma membrane SNARE protein that interacts with syntaxin 4, was not changed when syntaxin 4 was depleted (Fig. 1*F*).

Together, the data show that depletion of syntaxin 4 resulted in inhibition of basolateral and tight junction protein delivery. Apical targeting was not affected but the apical domain was greatly expanded.

Syntaxin 4 Knockdown Differentially Affects Basolateral Protein Delivery—Because our data indicated that basolateral localization of E-cadherin and β1-integrin was differentially affected by syntaxin 4 knockdown, we analyzed membrane transport and correct polarized delivery in more detail for several different basolateral proteins. For this, we quantified the localization of E-cadherin, β1-integrin, and Na,K-ATPase β1 using surface biotinylation. Surface biotinylation of E-cadherin showed that a small but significant portion of this protein was missorted to the apical surface (Fig. 2, *A, top blot, bottom, bar graph; open bars*, apical E-cadherin). However, the larger effect was seen in total delivery to the plasma membrane, as we found that the total surface biotinylation was reduced in syn4KD cells (Fig. 2*B, open bars*: surface-biotinylated protein as fraction of total immunoprecipitated protein, 73 ± 10% for syn4KD3).

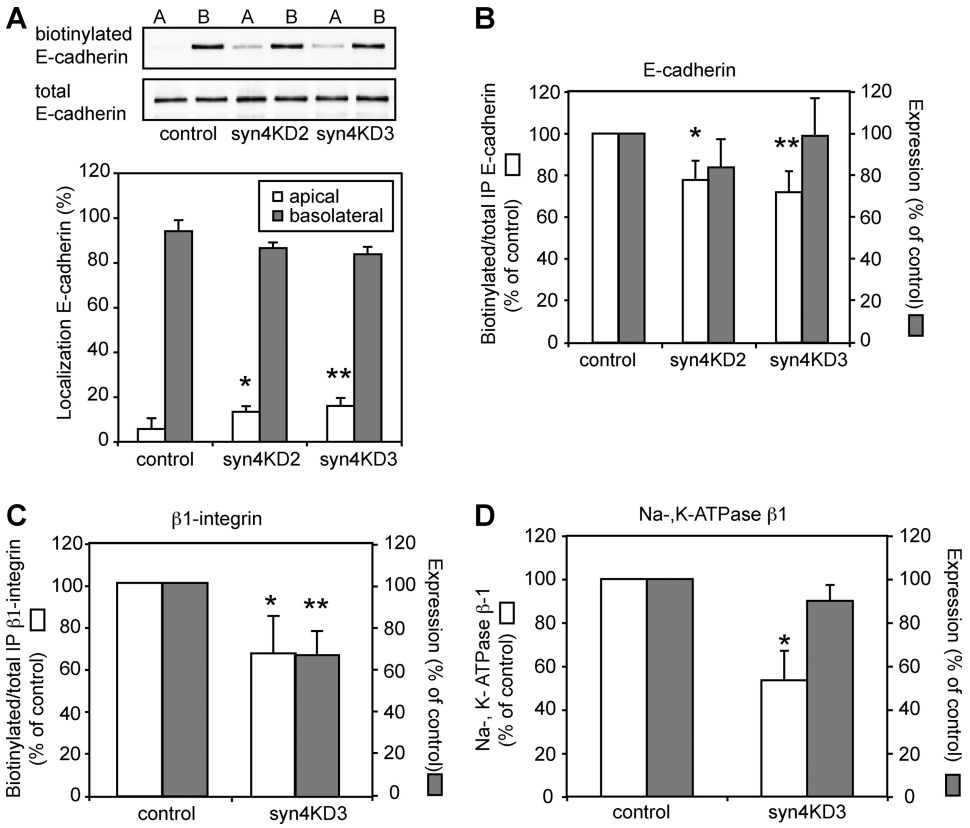

FIGURE 2. **Knockdown of syntaxin 4 results in intracellular accumulation of basolateral proteins.** The apical or basolateral membrane surface of syntaxin 4 knockdown and control cells were biotinylated and the extent of biotinylation was determined after immunoprecipitation of E-cadherin or β1-integrin. *A, top,* Western blots of biotinylated E-cadherin and total E-cadherin for control (LucKD), syn4KD2, and syn4KD3 cells. Note the small increase in apical E-cadherin for the knockdown cells. *Bottom*, biotinylated apical and basolateral E-cadherin was quantified as percentage of total biotinylated E-cadherin. Apical, *open bars*, basolateral, *closed bars*. These results are the mean of three independent experiments (*, $p < 0.01$; **, $p < 0.001$). *B,* biotinylated E-cadherin was quantified as the percentage of total immunoprecipitated E-cadherin and the results are normalized to control cells (*open bars*). These results are the mean of three independent experiments (*, $p < 0.005$; **, $p < 0.005$). The *closed bars* show expression levels of E-cadherin in lysates of control, syn4KD2, and syn4KD3 cells. *C,* biotinylated β1-integrin was quantified as percentage of total immunoprecipitated β1-integrin and the results are normalized to control cells (*open bars*). These results are the mean of three independent experiments (*, $p < 0.05$). The *closed bars* show expression levels of β1-integrin in lysates of control and syn4KD3 cells (**, $p < 0.001$). *D,* quantification of pulled down biotinylated Na,K-ATPase β1 and total Na,K-ATPase β1 in syn4KD3 as the percentage of control cells. The results are the mean ± S.D. of three independent experiments (*, $p < 0.05$).

When we repeated these experiments for β1-integrin, we also found a small but significant increase in apical localization (not shown). Total surface biotinylation of β1-integrin was substantially reduced (Fig. 2*C, open bars*: surface biotinylated protein as fraction of total immunoprecipitated protein, 68 ± 17%). Interestingly, we also found differences between the two proteins, as β1-integrin but not E-cadherin expression was significantly reduced in syn4KD3 cells compared with control cells (Fig. 2, *B, closed bars,* E-cadherin (98 ± 14%) *versus C, closed bars,* β1-integrin (66 ± 10%). Expression levels are indicated as a percentage of control). Finally, we analyzed basolateral localization of Na,K-ATPase β1 by surface biotinylation. In the syn4KD cells surface biotinylation was strongly reduced (Fig. 2*D*, *open bar*, 53 ± 13%) with little effect on protein expression level (Fig. 2*D*, *closed bar*, 90 ± 7%), suggesting that a considerable amount of the protein was localized intracellular.

Thus, when comparing the results of the different basolateral proteins we found that syntaxin 4 knockdown affects basolateral targeting of protein differently. Basolateral localization of E-cadherin was affected to a lesser extent compared with β1-integrin and Na,K-ATPase β1, in which syntaxin 4 knockdown results in intracellular protein accumulation with little apical mistargeting. These results are in agreement with the immunofluorescence data shown in Fig. 1*C*. Together, our data suggests that the loss of function of syntaxin 4 mainly results in failure to deliver proteins to the plasma membrane, rather than cause their missorting to the apical surface.

Accumulation of Intracellular Vesicles in syn4KD Cells—Our findings that syntaxin 4 knockdown inhibited the steady state localization of basolateral proteins at a different extent may be explained by differential stability of these proteins at the basolateral surface, rather then by differences in basolateral targeting. We therefore analyzed how syntaxin 4 knockdown affects trafficking of newly synthesized protein to the basolateral membrane. For this, we used live cell imaging of the temperature-sensitive mutant of the VSV-G protein (tsO45) tagged to EGFP. This mutation causes accumulation of the protein in the ER, whereas a subsequent incubation at 19.5 °C further accumulates the protein in the trans-Golgi network. We followed the synchronous transport of VSV-G-EGFP to the plasma membrane after removing the temperature block (33). In control cells an increase of lateral fluorescence was observed due to arrival of VSV-G-EGFP at the lateral membrane (Fig. 3*A*). This was accompanied by a decrease in intracellular fluorescence as

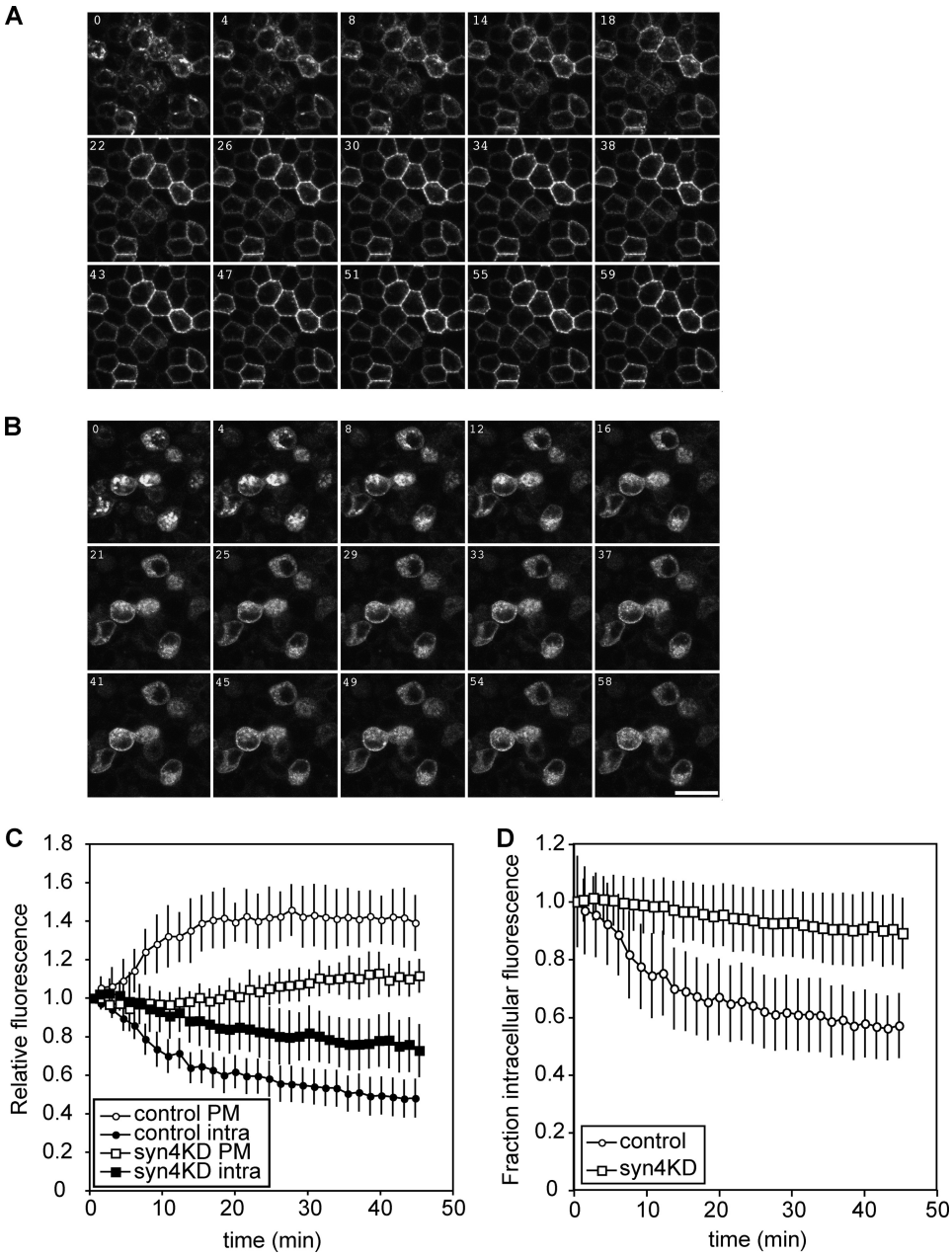

FIGURE 3. **Transport of VSV-G-EGFP tsO45 in control and syntaxin 4 knockdown cells.** Control cells (LucKD cells) and syn4KD3 cells were infected with adenovirus for VSV-G-EGFP tsO45 and incubated overnight at 39.5 °C. After 18 h, cells were incubated at 19.5 °C for 2 h and transferred to 32 °C. Transport of VSV-G-EGFP tsO45 was followed for 45 min and imaged using confocal microscopy. *A,* transport of VSV-G-EGFP tsO45 in control cells. *B,* transport of VSV-G-EGFP tsO45 in syn4KD3 cells. *Scale bar* is 20 μm. *C,* quantification of plasma membrane fluorescence (*open circles*, control cells; *open squares*, syn4KD cells) and intracellular fluorescence (*closed circles*, control cells; *closed squares*, syn4KD cells). The results are shown as mean ± S.D. of 12 individual cells. *D,* change of intracellular fluorescence for control and syn4KD3 cells as a fraction of total fluorescence (*open circles*, control cells; *open squares*, syn4KD3 cells).

VSV-G-EGFP is transported out of the trans-Golgi network. The delivery of VSV-G-EGFP to the plasma membrane was clearly inhibited in the syn4KD cells (Fig. 3*B*). Semiquantitative analysis of fluorescence of 12 individual control and syn4KD cells showed that maximum fluorescence at the plasma membrane was reached after 20 min in control cells (Fig. 3*C*, *open circles*). In the syn4KD cells, maximum fluorescence levels are reached after 40 min (*open squares*) and this fraction of fluorescence is ~30% compared with the control cells. This number is likely an overestimation as our system does not distinguish between actual plasma membrane localization and localization of transport vesicles close to the plasma membrane. Total intracellular fluorescence did not decrease in the syn4KD cells to the same level as the control cells (Fig. 3, *C*, *closed symbols*, and *D*). These data suggest that depletion of syntaxin 4 does not inhibit the exit of newly synthesized VSV-G-EGFP from the Golgi area, but does cause an accumulation of intracellular transport vesicles containing VSV-G-EGFP as a result of inhibition of membrane fusion.

Munc18c Knockdown Mimics the Syntaxin 4 Phenotype—Several studies have shown that expression levels of syntaxin 4 and munc18c are tightly linked (27, 28). To determine how expression of munc18c affects syntaxin 4 expression and localization in MDCK cells, cell lines depleted in munc18c were

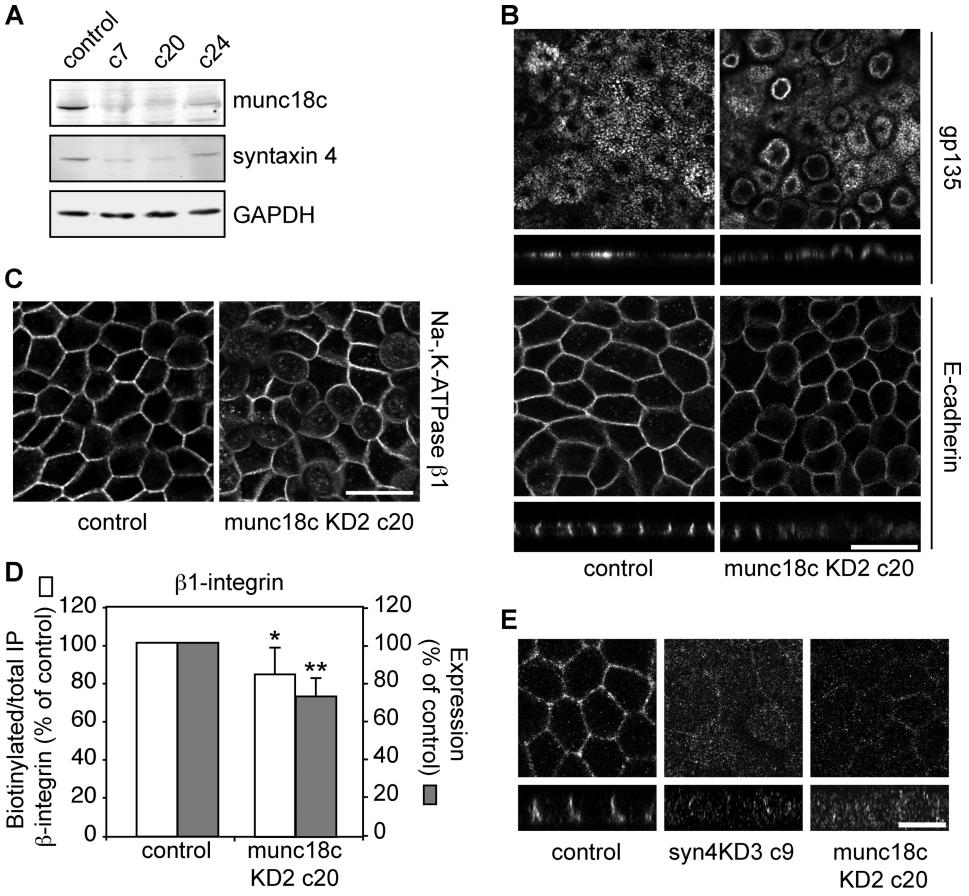

FIGURE 4. **Munc18c knockdown has a similar phenotype as syntaxin 4 depletion.** *A,* expression levels were determined by Western blotting of canine munc18c and syntaxin 4 in control and different clones of munc18c knockdown cells (*munc18cKD2*). GAPDH was used as a loading control. *B,* immunofluorescence of munc18c KD2 c20 and control cells (LucKD) grown for 5 days on filter. Cells were stained for gp135/podocalyxin (*top*, with *x-z* scans of gp135) and E-cadherin (*bottom*, with *x-z* scans of E-cadherin). *Scale bars* are 20 μm. *C,* immunofluorescence of munc18c KD2 c20 and control cells (LucKD) grown for 5 days on filter. Cells were stained for Na,K-ATPase β1. *Scale bar,* 20 μm. *D,* the relative biotinylation of total immunoprecipitated β1-integrin was quantified compared for control cells (LucKD) and munc18cKD c20 cells and the results are normalized to control cells (*open bars*). Relative expression levels of β1-integrin in lysates of control and munc18c KD c20 cells are shown as *closed bars*. The results are shown as a mean $\pm$ S.D. of three independent experiments (*, $p < 0.001$; **, $p < 0.001$). *E,* control (LucKD), syn4KD3 c9, and munc18c KD2 c20 stained for syntaxin 4. *Scale bar,* 10 μm.

made. Two of the 6 shRNA hairpins we tested gave a knockdown of $\pm$80% compared with a control vector upon transient transfection. We made cell lines using munc18cKD2 in which knockdown was about 80–90% (Fig. 4*A*) and found that munc18c knockdown reduced expression of syntaxin 4 expression (Fig. 4*A*). We were not able to stain for endogenous munc18c, using several different antibodies and fixation protocols. However, as Western blotting showed such significant reduction, it is likely that most of the cells were depleted in munc18c. Similar to what we observed in syn4KD cells, munc18cKD cells showed extended apical domains (Fig. 4*B*, munc18cKD2 c20, similar results were obtained with other clones). The localization of E-cadherin was not grossly affected (Fig. 4*B*), but both Na,K-ATPase β1 (Fig. 4*C*) and β1-integrin (not shown) showed increased intracellular staining and reduced staining at the lateral membrane. Using biotinylation studies we found that munc18c depletion resulted in reduced basolateral surface labeling of β1-integrin (Fig. 4*D*). Thus, the phenotype of these cell lines resembled syntaxin 4 knockdown cells. However, the phenotype of munc18c knockdown was less severe than observed for the syn4KD cells. When we stained for endogenous syntaxin 4 in munc18cKD cells we found, although difficult to detect, some residual basolateral staining (Fig. 4*E*).

The Phenotype of syn4KD Cells Does Not Depend on the Reduction of munc18c—Knockdown of syntaxin 4 results in a decrease of munc18c levels and vice versa. In the case of syntaxin 4 knockdown, the remaining levels of munc18c are about 40%. To determine whether the effects of syntaxin 4 knockdown on trafficking to the basolateral membrane is solely dependent on syntaxin 4 depletion, we restored expression levels of munc18c. For this we made a cell line that expresses FLAG-munc18c under a tet-repressible promotor (7) and is depleted in syntaxin 4. Expression of FLAG-munc18c in control cells (FLAG-munc18c) reduced endogenous levels of munc18c considerably (Fig. 5*A*). A likely explanation is that munc18c is only stable when bound to syntaxin 4. As overexpressed FLAG-munc18c participates in the pool of munc18c that can bind syntaxin 4, endogenous levels are therefore reduced.

The FLAG-munc18c-syn4KD3 cells had a similar phenotype as the syntaxin 4 knockdown cells. Claudin 2 and Na,K-ATPase β1 showed significant intracellular localization (Fig. 5*B*) and expression of FLAG-munc18c did not affect this intracellular localization. These cells also showed the extended apical domain when FLAG-munc18c is expressed (Fig. 5*C*). Localization of claudin 2 or Na,K-ATPase β1 in the FLAG-munc18c

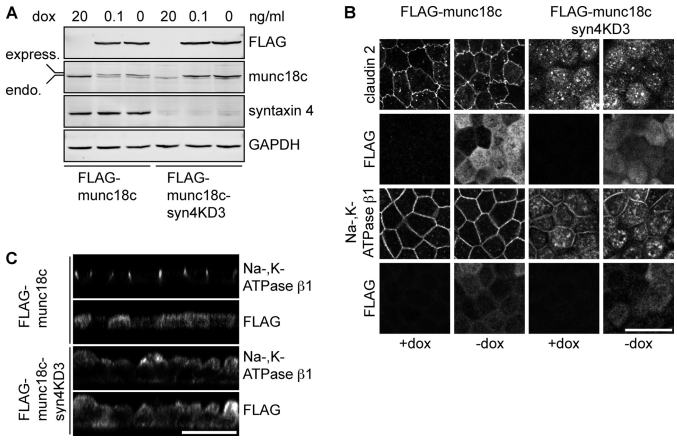

FIGURE 5. **Reduced munc18c expression does not contribute to syntaxin 4 knockdown phenotype.** Syntaxin 4 was depleted in cells that inducibly express mouse FLAG-munc18c under control of the Tet-off system (FLAG-munc18c-syn4KD3 cells). *A,* expression levels of endogenous munc18c, FLAG-munc18c, and syntaxin 4 were determined by Western blotting. GAPDH was used as a loading control. Two different dox concentrations were used to regulate FLAG-munc18c expression. Please note the reduction of endogenous munc18c in the parental FLAG-munc18c cells when FLAG-munc18c is expressed. Also note that syntaxin 4 expression stays repressed in the presence of FLAG-munc18c. *B,* FLAG-munc18c and FLAG-munc18c-syn4KD3 cells were grown for 5 days on filter in the presence or absence of dox, fixed, and stained for claudin 2, Na,K-ATPase β1, and FLAG. This image shows a projection of *x-y* images. *C,* FLAG-munc18c and FLAG-munc18c-syn4KD3 cells were grown for 5 days on filter, fixed, and stained for Na,K-ATPase β1 and FLAG. This image shows a *x-z* scan. *Scale bars,* 20 μm.

was not affected by FLAG-munc18c expression. Expression levels of syntaxin 4 levels remained low when FLAG-munc18c expression was induced (Fig. 5*A*, *FLAG-munc18c syn4KD3*). These results show that syntaxin 4 expression is essential for basolateral delivery of proteins and that the reduced levels of munc18c do not contribute to the observed phenotype of the syn4KD cells.

N-terminal Region of Syntaxin 4 Contains Basolateral Sorting Signal—We recently showed that exchanging the first N-terminal 40 amino acids of syntaxin 3 with those of syntaxin 4 results in complete basolateral localization of syntaxin 3 (7). As this suggests that the N-terminal sequence of syntaxin 4 contains basolateral sorting signals, we further characterized these signals by making several deletion mutants of rat syntaxin 4. To visualize the mutants we ecto-tagged syntaxin 4 with EGFP at the C terminus (supplemental Fig. S2*A*). Ecto-tagging SNARE proteins at the C terminus does not effect the localization and function of these proteins (34, 35). Indeed, wild type (WT) EGFP-tagged syntaxin 4 showed a similar lateral localization as untagged syntaxin 4. We and others have previously shown the importance of the first 8 amino acids of the N-terminal sequence for munc18c binding (7, 36, 37). However, transient expression of syntaxin 4 with N-terminal deletions up to 15 amino acids had no major effects on the localization of syntaxin 4 (Fig. 6*A*), although removal of the first 10 amino acids completely blocked binding to munc18c (see below, Fig. 7*A*). This suggests that basolateral targeting of syntaxin 4 is independent of munc18c binding.

Additional deletion of amino acids caused intracellular localization of syntaxin 4 (Δ20, Δ30, and Δ40), although a significant amount was still directed to the lateral membrane. Less cells express syntaxin 4-Δ20, -Δ30, and -Δ40 expression, which is

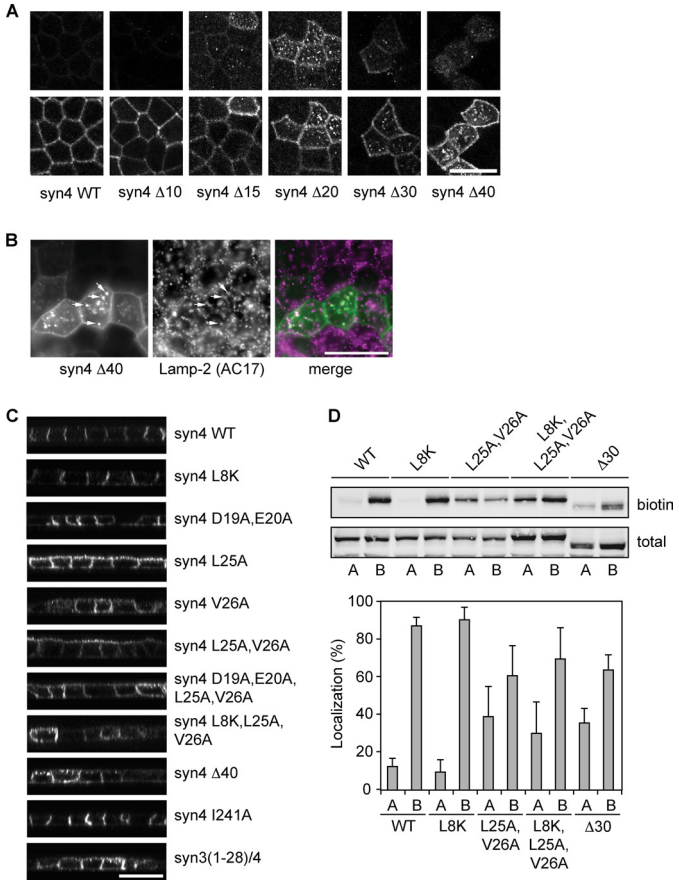

FIGURE 6. **The N-terminal region of syntaxin 4 contains a basolateral sorting signal.** *A,* localization of different deletion mutants in polarized MDCK cells. The different mutants were visualized by staining for GFP. *Top images* are the apical section and *bottom images* are the basolateral sections. *B,* co-localization of syn4-Δ40 mutant with lysosomes. Cells were stained for GFP and Lamp-2, a marker for lysosomes. *C,* localization of several mutants of syntaxin 4 in polarized MDCK cells. Cells were fixed and stained for GFP. *x-z* scans of the images are shown. *D,* localization of syntaxin 4-WT and some syntaxin 4 mutants determined by domain-specific biotinylation at the apical or basolateral membranes. Cells were biotinylated and the biotinylated protein was pulled down using Neutravidin and analyzed by Western blotting with an antibody to syntaxin 4. *Top panel* shows Western blot. *Bottom panel* shows the quantification of apical (*A*) and basolateral (*B*) localized syntaxin 4 as a percentage of total. The results are shown as the mean ± S.D. of five independent experiments (the difference in localization between syntaxin 4-WT and syntaxin 4-L25A,V26A, -L8K,L25A,V26A, or -Δ30 were all significant with $p < 0.01$). *Scale bars,* 20 μm.

likely caused by degradation. Indeed, intracellular syntaxin 4-Δ40 co-localized with the endosomal/lysosomal protein Lamp-2 (Fig. 6*B*) (21).

Together our results indicate that a sorting signal is present in the region just after the first 15 amino acids. We determined that amino acids Leu-25 and Val-26 are conserved among different species (supplemental Fig. 2*C*). Introduction of a V26A, and to a lesser extent L25A mutation, resulted in significant apical localization, but no significant intracellular staining (Fig. 6*C*). Other mutations of the acidic amino acids located in the 15–20-amino acid region of syntaxin 4 had little effect on its localization (Fig. 6*C* and supplemental Fig. S2*B*). This is unexpected as deletion of this region resulted in intracellular localization (Fig. 6*A*).

To exclude any effect of the EGFP tag, we also analyzed cells stably expressing C-terminal myc-tagged syntaxin 4 WT and

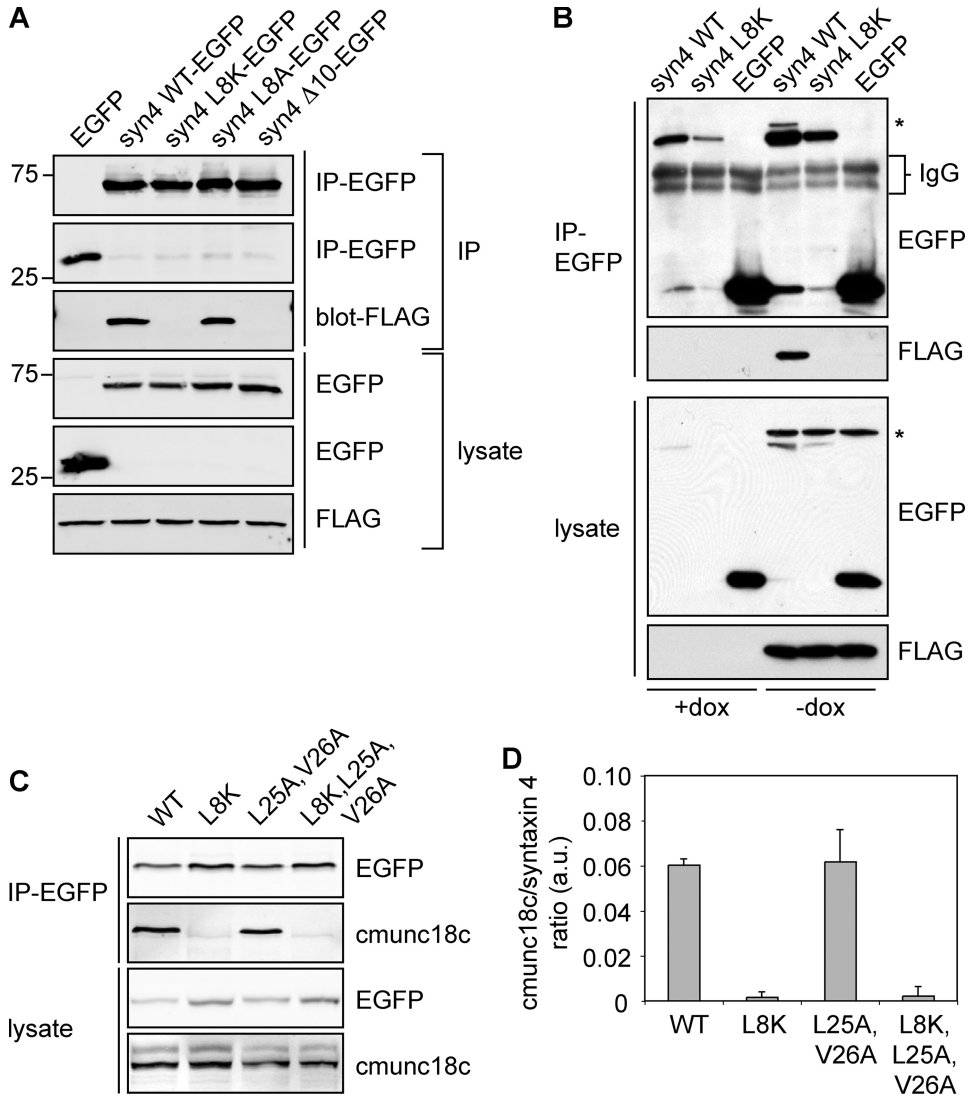

FIGURE 7. **Basolateral sorting motif in syntaxin 4 is independent of munc18c binding sequence.** *A,* FLAG-munc18c cells were nucleofected with constructs for expression of EGFP or syntaxin 4 WT-EGFP or different syntaxin 4 mutants (syntaxin 4-L8K-EGFP, syntaxin 4-L8A-EGFP, and syntaxin 4-Δ10-EGFP). EGFP and the different syntaxin 4 proteins were immunoprecipitated with a GFP antibody and co-immunoprecipitated (*IP*) FLAG-munc18c was detected with a FLAG antibody. *B,* FLAG-munc18c cells in the presence or absence of dox were nucleofected with syntaxin 4-WT-EGFP, syntaxin 4-L8K-EGFP, and EGFP. EGFP and syntaxin 4-EGFP constructs were immunoprecipitated (*IP*) and co-immunoprecipitated FLAG-munc18c was visualized. *Star* indicates residual FLAG-munc18c that was not stripped off. IgG bands have been indicated. *C,* syntaxin 4 proteins were immunoprecipitated with a GFP antibody and co-immunoprecipitated endogenous munc18c (*cmunc18c*) was detected using a canine-specific munc18c antibody. *D,* quantification of co-immunoprecipitated munc18c, normalized for the amount of immunoprecipitated syntaxin 4. The results are the mean ± S.D. of three independent experiments.

mutants and found a similar apical localization (supplemental Fig. S3*A*) for syntaxin 4-L25A,V26A. Mutations in EGFP that prevent dimerization (A206K) (38) or oligomerization (C49S) (39) did not change the localization of syntaxin 4-WT or syntaxin 4-L25A,V26A (supplemental Fig. S3*B*). Thus, Leu-25 and Val-26 are important for correct localization of syntaxin 4. We confirmed this finding in several other epithelial cells, including Fisher rat thyroid cells and LLC-PK1 cells (supplemental Fig. S3*C*).

Interestingly, the deletion mutants of syntaxin 4 localized partly intracellular, whereas the L25A,V26A mutant was missorted to the apical surface, but did not accumulate intracellularly. This suggests that an additional sorting determinant is present in the N-terminal region. Because the L25A,V26A mutant, but not deletion mutants binds munc18c, we investigated if munc18c is involved in the localization of syntaxin 4. For this, we introduced the L8K mutation, which decreases munc18c binding (10). This mutant showed a normal lateral localization (Fig. 6*C*). However, mutation of both the sorting sequence and the munc18c binding peptide (L8K, L25A, and V26A) showed a non-polarized localization and high expressing cells showed intracellular staining (Fig. 6*C* and supplemental Fig. S3*D*). The localization of this mutant resembled deletion mutants Δ20-Δ40 and the syn3/4 chimera, suggesting that N-terminal peptide binding of munc18c contributes to correct localization of syntaxin 4.

To analyze the apical and basolateral steady state localization by cell surface biotinylation, we generated syntaxin 4 mutants as described above with an extracellular EGFP tag. We expressed these under control of the tet-inducible system (40), which allowed us to obtain similar expression levels of the different constructs (Fig. 6*D*). Expression of EGFP-tagged syn-

taxin 4-WT, syntaxin 4-L8K, syntaxin 4-L25A,V26A, syntaxin 4-L8K,L25A,V26A, and syntaxin 4-Δ30 did not affect polarized cell morphology and the EGFP-tagged proteins localized similarly to the transiently expressed constructs (not shown). Consistent with our immunofluorescence data, there was a significant increase of apical syntaxin 4-L25A,V26A, syntaxin 4-L8K,L25A,V26A, and syntaxin 4-Δ30 as compared with syntaxin 4-WT, whereas no significant changes were observed for syntaxin 4-L8K (Fig. 6*D*).

Together, our results show that residues Leu-25 and Val-26 within the N-terminal region are required for correct basolateral localization and act by a munc18c-independent mechanism. Our data, furthermore, indicates that munc18c plays a separate role in the polarized localization of syntaxin 4.

L25A,V26A Mutation in Syntaxin 4 Does Not Affect Munc18c Binding—Recent published crystal structure data showed that only the first 12 amino acids of the N-terminal peptide of syntaxin 4 bind to munc18c (36). To confirm this, and to exclude that the L25A,V26A mutation inhibited binding, we transiently expressed different syntaxin 4-EGFP constructs or the pEGFP-N1 control vector in MDCK cells that express FLAG-tagged munc18c in a tet-regulatory manner (7). FLAG-munc18c co-immunoprecipitated with syntaxin 4-WT but not with syntaxin 4-L8K, syntaxin 4-Δ10, or the control EGFP (Fig. 7*A*), thus confirming previous reported results (10). Even with longer exposure times we did not observe any co-immunoprecipitation between syntaxin 4-L8K or syntaxin 4-Δ10 with munc18c. Despite the fact that syntaxin 4-L8K and FLAG-munc18c do not interact, co-expression of FLAG-munc18c increased expression of both syntaxin 4 WT and 4-L8K (Fig. 7*B*).

Both syntaxin 4-WT and syntaxin 4-L25A,V26A, but not syntaxin 4-L8K or syntaxin 4-L8K,L25A,V26A also interacted with endogenous canine munc18c (cmunc18c, Fig. 7, *C* and *D*). This was confirmed by reciprocal co-immunoprecipitations using transiently transfected syntaxin mutants (supplemental Fig. S4). These residues (Leu-25 and Val-26) are not required for munc18c binding but replacing Leu-8 with lysine or deletion of 10 amino acids of the N-terminal region resulted in complete loss of munc18c binding.

Munc18c Stabilizes Syntaxin 4 at Plasma Membrane—To examine if munc18c knockdown affected syntaxin 4-localization we nucleofected control or munc18c knockdown cells (munc18cKD2 c20) with syntaxin 4-WT and syntaxin 4-L25A,V26A. Consistent with the basolateral localization of the syntaxin 4-L8K mutant, munc18c knockdown did not affect syntaxin 4-WT localization (Fig. 8*A*). However, depletion of munc18c caused syntaxin 4-L25A,V26A to localize exclusively lateral as compared with the non-polarized localization in the control cells (Fig. 8*B*). A possible explanation is that munc18c binding to syntaxin 4-L25A,V26A may mask a potential apical endocytosis signal and depletion of munc18c allows apical syntaxin 4-L25A,V26A to be endocytosed. It is expected that syntaxin 4-L25A,V26A expressed in munc18cKD cells localize also intracellularly as observed for the syntaxin 4-L8K,L25A,V26A mutant (Fig. 6*C*). This is, however, not the case and this is likely the result of insufficient expression levels to detect intracellular syntaxin 4-L25A,V26A.

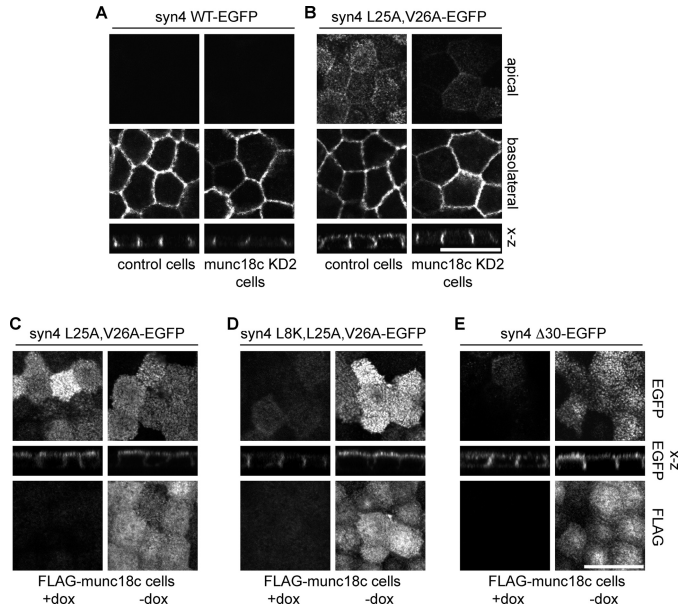

FIGURE 8. **Munc18c is required for apical localization of syntaxin 4-L25A,V26A.** *A,* localization of syntaxin 4-WT-EGFP in control and munc18cKD2 c20 cells. *B,* localization of syntaxin 4-L25A,V26A-EGFP in control and munc18cKD2 c20 cells. Apical, basolateral, and *z*-sections are shown. *C,* localization of syntaxin 4-L25A,V26A in control (+*dox*) and FLAG-munc18c expressing cells (−*dox*). *D,* localization of syntaxin 4-L8K,L25A,V26A in control (+*dox*) and FLAG-munc18c expressing cells (−*dox*). *E,* localization of syntaxin 4-Δ30 in control (+*dox*) and FLAG-munc18c expressing cells (−*dox*). *Top panels* and *z*-section shows EGFP and the *bottom panels* show FLAG staining. *Scale bars,* 20 μm.

We next examined if munc18c contributes to the apical localization of syntaxin 4-L25A,V26A. For this we used the cell line that expresses FLAG-munc18c under a tet-inducible promoter. Overexpression of munc18c results in increased levels of ectopically expressed syntaxin 4 (see Fig. 7*B*) (7). As expected, transiently expressed syntaxin 4-L25A,V26A in cells that do not express FLAG-munc18c (+dox) localized partially apically (Fig. 8*C*, +*dox*). Induction of FLAG-munc18c expression (−*dox*) increased the expression levels, but did not alter the localization of syntaxin 4-L25A,V26A (Fig. 8*C*, −*dox*). In contrast, expression of syntaxin 4-L8K,L25A,V26A or syntaxin 4-Δ30 in FLAG-munc18c expressing cells resulted in significant apical localization and an increased expression of this mutant as compared with cells that do not express FLAG-munc18c (Fig. 8, *D* and *E*, compare +*dox* to −*dox*). This was unexpected because we were not able to find any interaction between FLAG-munc18c and syntaxin 4-L8K,L25A,V26A or syntaxin 4-Δ30 by immunoprecipitation studies (Fig. 7 and supplemental Fig. S4 and data not shown). Without FLAG-munc18c expression (+dox), syntaxin 4-Δ30 and -Δ40 localized partly intracellularly. In FLAG-munc18c expressing cells (−dox) no intracellular staining was observed (supplemental Fig. S5, *C* and *D*, +*dox*). Nevertheless, these data show that munc18c overexpression increases syntaxin 4-L25A,V26A localization at the apical membrane.

Binding of munc18c Is Not Essential for Rescue of Basolateral Transport in Syntaxin 4 Knockdown Cells—We show that specific mutations of syntaxin 4 in the N-terminal region resulted in mislocalization of syntaxin 4. We next examined if these syntaxin 4 mutants were still able to function in protein deliv-

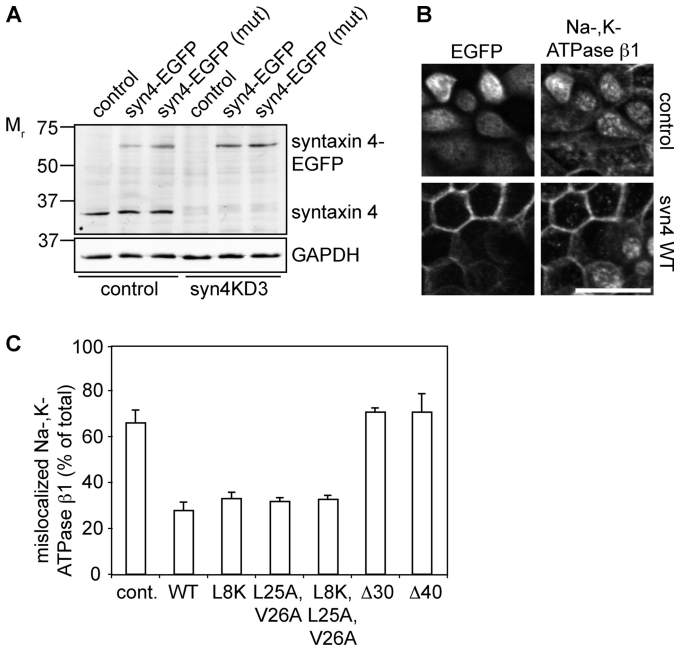

FIGURE 9. **Expression of syntaxin 4-WT and mutants rescue basolateral localization of Na,K-ATPase β1.** *A,* Western blot shows expression levels of endogenous (*syntaxin 4*) and nucleofected syntaxin 4 (*syntaxin 4-EGFP*) in control cells and syn4KD3 cells. Syntaxin 4-WT-EGFP (*syn4-EGFP*) and syntaxin 4 with silent mutations in the region to which the hairpin is directed in canine syntaxin 4 (*syn4-EGFP mut*). GAPDH was used as a loading control. *B,* control cells (LucKD) and syn4KD3 cells were nucleofected with EGFP or syntaxin 4-WT-EGFP and stained for EGFP and Na,K-ATPase β1. Please note the intracellular localization of Na,K-ATPase β1 in cells without syntaxin 4-WT-EGFP expression. *Scale bar,* 20 μm. *C,* quantification of mislocalized Na,K-ATPase β1 in syn4KD3 cells expressing EGFP (cont.), syntaxin 4-WT-EGFP (*WT*), syntaxin 4-L8K-EGFP (*L8K*), syntaxin 4-L25A,V26A-EGFP (*L25A,V26A*), syntaxin 4-L8K,L25A,V26A-EGFP (*L8K,L25A,V26A*), syntaxin 4-Δ30 (*Δ30*), and syntaxin 4-Δ40 (*Δ40*). The results are the mean ± S.D. of three independent experiments (significant for syntaxin 4-WT-EGFP, syntaxin 4-L8K-EGFP, syntaxin 4-L25A,V26A-EGFP, and syntaxin 4-L8K,L25A,V26A-EGFP constructs compared with control (*cont.*), $p < 0.01$).

ery. Therefore we expressed syntaxin 4-WT (species is rat) in syn4KD cells. Canine and rat syntaxin 4 showed a 16-nucleotide overlap in the sequence that was targeted for knockdown. Yet expression of rat syntaxin 4 was not reduced in syn4KD cells compared with control cells. Also endogenous syntaxin 4 levels are still reduced when rat syntaxin is expressed. Expression of rat syntaxin 4 with silent mutations in the sequence to make it refractory to the hairpin gave similar results (Fig. 9*A*). Expression of syntaxin 4-WT completely rescued the phenotype of the syn4KD cells (Fig. 9*B* and supplemental Fig. S6*A*) and resulted in cells with normal morphology and no intracellular Na,K-ATPase β1. Expression of EGFP did not result in any rescue (Fig. 9*B*).

We next analyzed the localization of Na,K-ATPase β1 in syn4KD cells expressing syntaxin 4-WT or the different mutants. Intracellular and membrane-localized fluorescence was quantified of projections of stacks (supplemental Fig. S6*B*). It is important to point out that the relative amount of intracellular fluorescence is underestimated as we quantify plasma membrane fluorescence of two bordering cells. We observed in all mutants, except syntaxin 4-Δ30 and -Δ40, an increase of Na,K-ATPase β1 localization at the membrane. This suggests that binding of munc18c to the syntaxin 4 N terminus is not required for the function of syntaxin 4. However, additional residues are present in the N terminus that are essential for the function of syntaxin 4 as syntaxin 4-Δ30 and -Δ40 were not able to rescue Na,K-ATPase transport. In the case of apical localized syntaxin 4-L25A,V26A, we did not observe any mislocalization of Na,K-ATPase β1 to the apical membrane (supplemental Fig. S6*C*). These results show that munc18c binding to syntaxin 4 *per se* is not required for the function of syntaxin 4 in basolateral trafficking in MDCK cells yet the N terminus contains residues that are important for its function.

DISCUSSION

We show that depletion of syntaxin 4 results in intracellular accumulation of basolateral and tight junction proteins. All basolateral proteins we tested so far show decreased basolateral targeting in the syn4KD cells, although E-cadherin was less sensitive to the loss of syntaxin 4 compared with the other basolateral proteins. This would be in agreement with the function of E-cadherin as an initiator of basolateral polarity and acting upstream in the biogenesis of basolateral polarity (41). Also, E-cadherin at the plasma membrane will likely be stabilized by trans-interactions. Intracellular E-cadherin accumulation increased in cells grown for longer periods on filter, indicating that recycling of E-cadherin after establishment of polarity is affected by depletion of syntaxin 4. Delivery of claudin 2 and occludin is also inhibited by syntaxin 4 depletion, indicating that syntaxin 4 is also involved in the delivery of these tight junction proteins. However, we find no effect on the permeability for small molecules in syn4KD cells compared with control cells, suggesting that not all tight junction components are affected by syntaxin 4 knockdown. This is also apparent from the unchanged localization of ZO-1. Despite reduced basolateral delivery, cells maintain their polarity and only a small fraction of the tested proteins were found to localize at the apical domain.

We examined the basolateral targeting of syntaxin 4 and identified residue Leu-25 and to a lesser extent Val-26 as essential for basolateral sorting of syntaxin 4. These residues resemble a dileucine motif, preceded by a region of acidic residues. Dileucine motifs act as endocytosis signals, but can also act as basolateral target signals (2, 42). The motif in rat and mouse syntaxin 4 differs from the consensus dileucine motif, as the first acidic amino acid is at the −5 and not −4 position relative to the first leucine (see supplemental Fig. S2*C*). Mutations of these acidic residues in syntaxin 4 do not affect basolateral sorting. However, a truncation including the acidic residues but not the leucine/valine motif caused missorting (Fig. 7*A*, *syn4-Δ20*). This is similar to what was previously reported for the sorting of CD147, in which removal of acidic amino acids resulted in apical missorting but substitution of these residues with alanine did affect trafficking (43). Dileucine motifs can bind the μ, β, or γ/σ1 subunits of AP1, the adaptor involved in the trans-Golgi network to plasma membrane transport (42, 44–46). MDCK cells express the epithelial specific adaptor subunit μ1B and it was shown that this subunit is essential for the correct sorting of some basolateral proteins (47, 48). However, in LLC-PK1 cells, a cell line that does not express μ1B (48), syntaxin 4 localizes mostly basolateral. Also, the L25A,V26A mutant shows increased apical localization in this cell line

suggesting that μ1B is not directly involved in sorting of syntaxin 4 to the basolateral membrane.

It is still unclear if munc18 proteins contribute to syntaxin localization. One study showed that syntaxin 1A was targeted correctly in munc18-1-deficient mice (49). However, other studies found that knockdown of munc18-1/-2 in PC12 cells resulted in decreased expression and intracellular mislocalization of syntaxin 1A (50, 51).

In our system, knockdown of munc18c does not interfere with targeting of syntaxin 4 to the plasma membrane. Syntaxin 4 localization is also not affected by the introduction of deletions Δ10 and Δ15 or a mutation (L8K) that affects binding to munc18c. On the other hand, although the L25A,V26A mutation is missorted, it does not affect munc18c binding. From these results we conclude that munc18c is not required for syntaxin 4 targeting to the plasma membrane. However, removal of the first 20 amino acids of the N terminus of syntaxin 4 or introducing mutations that affect both munc18c binding and plasma membrane sorting (L8K,L25A,V26A) results in intracellular localization of syntaxin 4. This suggests that munc18c stabilizes syntaxin 4 at the plasma membrane.

Indeed, depletion of munc18c results in reduced expression of syntaxin 4 or vice versa. Also the L8K mutation in syntaxin 4 affects its stability, as the expression of this mutant was lower after transient nucleofection compared with syntaxin 4-WT cells. In addition, overexpression of munc18c results in a decrease of endogenous munc18c. This suggests that munc18c levels are tightly controlled. Such a close interdependence of munc18c- and syntaxin 4-expression has been reported before (27, 28) and was also shown for other plasma membrane SNAREs (49, 52).

Membrane stabilization of syntaxin 4 by munc18c may also explain our localization studies of the syntaxin 4-L25A,V26A mutant. Syntaxin 4-L25A,V26A expression in munc18c-depleted cells results in reduced apical localization. Similarly, the munc18c binding mutant L8K,L25A,V26A is not localized at the apical membrane. However, munc18c overexpression results in stabilization of the L8K,L25A,V26A mutant and Δ30 and Δ40 deletion mutants at the apical membrane. This is an unexpected result because co-immunoprecipitation studies showed no interaction between munc18c and any of the L8K and deletion mutants, in both control and munc18c overexpressing systems (Fig. 8). Several explanations for this discrepancy are possible. The interaction of the L8K mutant with munc18c may be weak and lost during co-immunoprecipitation. Indeed, residual interaction between syntaxin 4 mutated in the N-peptide has been reported, as Latham and co-workers (10) found some interaction between syntaxin 4-L8K pulled down with munc18c-GST munc18c. Using FRET analysis it has been shown that another syntaxin 4 N-peptide mutant deficient in munc18c binding interacts *in vivo* with munc18c (37). Also, we have previously shown that syntaxin 4 without the N-terminal peptide binds munc18c (7) *in vitro*. Another possible explanation is that syntaxin 4 N-peptide mutants are part of a larger complex of syntaxins. It was recently shown that both syntaxin 1A and syntaxin 4 form large clusters of syntaxins, via interactions of their core regions (54, 55). The syntaxin 4-L8K could be localized together with endogenous syntaxins in clusters and these clusters may be stabilized by overexpression of munc18c that is bound to endogenous syntaxin.

Absence of munc18c interaction does not affect the function of syntaxin 4 in our system. Expression of syntaxin 4-L8K in syntaxin 4-depleted cells rescues Na,K-ATPase β1 localization to a similar extent as syntaxin 4-WT. Also, the effect of munc18c knockdown on delivery of basolateral proteins is not as pronounced as for syntaxin 4 and may rather be the effect of reduced syntaxin 4 levels.

Interestingly, syntaxin 4 mutant with a deletion of the first 30 residues did not rescue Na,K-ATPase β1 localization in the syntaxin 4 knockdown cells. This suggests that other residues in this region may be important for the function of syntaxin 4.

Taken together our data suggest that in epithelial cells, munc18c binding to the N-terminal peptide may not be essential for docking and fusion. Nevertheless, these results show the importance of stabilization of syntaxin 4 at the plasma membrane.

Depletion of syntaxin 4 causes intracellular accumulation of basolateral proteins but no substantial missorting to the apical membrane. Expression of the apical sorted syntaxin 4 mutant L25A,V26A in syntaxin 4-depleted cells does not result in mislocalization of Na,K-ATPase β1. This suggests that apical localization of syntaxin 4 is not sufficient to redirect trafficking of basolateral proteins. It is likely that specific combinations of SNAREs, tethering proteins, and other proteins (53, 56) will provide specificity in membrane fusion. How the different proteins of the tethering/fusion machinery interact and how this is regulated is still an open question. Further studies will be required to identify such combinations of protein complexes for the different trafficking pathways.

Acknowledgment—We thank Dr. J. Chernoff for reagents.

REFERENCES

1. Rodriguez-Boulan, E., Kreitzer, G., and Müsch, A. (2005) *Nat. Rev. Mol. Cell Biol.* **6,** 233–247
2. Mellman, I., and Nelson, W. J. (2008) *Nat. Rev. Mol. Cell Biol.* **9,** 833–845
3. Low, S. H., Chapin, S. J., Weimbs, T., Kömüves, L. G., Bennett, M. K., and Mostov, K. E. (1996) *Mol. Biol. Cell* **7,** 2007–2018
4. Gaisano, H., Ghai, M., Malkus, P., Sheu, L., Bouquillon, A., Bennett, M. K., and Trimble, W. S. (1996) *Mol. Biol. Cell* **7,** 2019–2027
5. Torkko, J. M., Manninen, A., Schuck, S., and Simons, K. (2008) *J. Cell Sci.* **121,** 1193–1203
6. Low, S. H., Chapin, S. J., Wimmer, C., Whiteheart, S. W., Kömüves, L. G., Mostov, K. E., and Weimbs, T. (1998) *J. Cell Biol.* **141,** 1503–1513
7. ter Beest, M., Chapin, S. J., Avrahami, D., and Mostov, K. E. (2005) *Mol. Biol. Cell* **16,** 5784–5792
8. Sharma, N., Low, S. H., Misra, S., Pallavi, B., and Weimbs, T. (2006) *J. Cell Biol.* **173,** 937–948
9. Wang, Z., and Thurmond, D. C. (2009) *J. Cell Sci.* **122,** 893–903
10. Latham, C. F., Lopez, J. A., Hu, S. H., Gee, C. L., Westbury, E., Blair, D. H., Armishaw, C. J., Alewood, P. F., Bryant, N. J., James, D. E., and Martin, J. L. (2006) *Traffic* **7,** 1408–1419
11. Hou, J., and Pessin, J. (2007) *Curr. Opin. Cell Biol.* **19,** 466–473
12. Toonen, R. F., and Verhage, M. (2007) *Trends Neurosci.* **30,** 564–572
13. Cosen-Binker, L. I., Morris, G. P., Vanner, S., and Gaisano, H. Y. (2008) *World J. Gastroenterol.* **14,** 2314–2322
14. Burgoyne, R. D., Barclay, J. W., Ciufo, L. F., Graham, M. E., Handley, M. T., and Morgan, A. (2009) *Ann. N.Y. Acad. Sci.* **1152,** 76–86
15. Südhof, T. C., and Rothman, J. E. (2009) *Science* **323,** 474–477

16. Jewell, J. L., Oh, E., and Thurmond, D. C. (2010) *Am. J. Physiol. Regul. Integr. Comp. Physiol.* **298,** R517–531
17. Yu, W., Datta, A., Leroy, P., O'Brien, L. E., Mak, G., Jou, T. S., Matlin, K. S., Mostov, K. E., and Zegers, M. M. (2005) *Mol. Biol. Cell* **16,** 433–445
18. Anderson, J. M., Stevenson, B. R., Jesaitis, L. A., Goodenough, D. A., and Mooseker, M. S. (1988) *J. Cell Biol.* **106,** 1141–1149
19. Balcarova-Ständer, J., Pfeiffer, S. E., Fuller, S. D., and Simons, K. (1984) *EMBO J.* **3,** 2687–2694
20. Herzlinger, D. A., and Ojakian, G. K. (1984) *J. Cell Biol.* **98,** 1777–1787
21. Nabi, I. R., Le Bivic, A., Fambrough, D., and Rodriguez-Boulan, E. (1991) *J. Cell Biol.* **115,** 1573–1584
22. van de Wetering, M., Oving, I., Muncan, V., Pon Fong, M. T., Brantjes, H., van Leenen, D., Holstege, F. C., Brummelkamp, T. R., Agami, R., and Clevers, H. (2003) *EMBO Rep.* **4,** 609–615
23. Chen, X., and Macara, I. G. (2006) *Methods Enzymol.* **406,** 362–374
24. Luton, F. (2005) *Methods Enzymol.* **404,** 332–345
25. Wakabayashi, Y., Chua, J., Larkin, J. M., Lippincott-Schwartz, J., and Arias, I. M. (2007) *Histochem. Cell Biol.* **127,** 463–472
26. Thévenaz, P., Ruttimann, U. E., and Unser, M. (1998) *IEEE Trans. Image Process.* **7,** 27–41
27. Yang, C., Coker, K. J., Kim, J. K., Mora, S., Thurmond, D. C., Davis, A. C., Yang, B., Williamson, R. A., Shulman, G. I., and Pessin, J. E. (2001) *J. Clin. Invest.* **107,** 1311–1318
28. Kanda, H., Tamori, Y., Shinoda, H., Yoshikawa, M., Sakaue, M., Udagawa, J., Otani, H., Tashiro, F., Miyazaki, J., and Kasuga, M. (2005) *J. Clin. Invest.* **115,** 291–301
29. Malliri, A., van Es, S., Huveneers, S., and Collard, J. G. (2004) *J. Biol. Chem.* **279,** 30092–30098
30. Füllekrug, J., Shevchenko, A., Shevchenko, A., and Simons, K. (2006) *BMC Biochem.* **7,** 8
31. Humbert, P. O., Dow, L. E., and Russell, S. M. (2006) *Trends Cell Biol.* **16,** 622–630
32. Navarro, C., Nola, S., Audebert, S., Santoni, M. J., Arsanto, J. P., Ginestier, C., Marchetto, S., Jacquemier, J., Isnardon, D., Le Bivic, A., Birnbaum, D., and Borg, J. P. (2005) *Oncogene* **24,** 4330–4339
33. Toomre, D., Keller, P., White, J., Olivo, J. C., and Simons, K. (1999) *J. Cell Sci.* **112,** 21–33
34. Steegmaier, M., Lee, K. C., Prekeris, R., and Scheller, R. H. (2000) *Traffic* **1,** 553–560
35. Sieber, J. J., Willig, K. I., Heintzmann, R., Hell, S. W., and Lang, T. (2006) *Biophys. J.* **90,** 2843–2851
36. Hu, S. H., Latham, C. F., Gee, C. L., James, D. E., and Martin, J. L. (2007) *Proc. Natl. Acad. Sci. U.S.A.* **104,** 8773–8778
37. D'Andrea-Merrins, M., Chang, L., Lam, A. D., Ernst, S. A., and Stuenkel, E. L. (2007) *J. Biol. Chem.* **282,** 16553–16566
38. Zacharias, D. A., Violin, J. D., Newton, A. C., and Tsien, R. Y. (2002) *Science* **296,** 913–916
39. Jain, R. K., Joyce, P. B., Molinete, M., Halban, P. A., and Gorr, S. U. (2001) *Biochem. J.* **360,** 645–649
40. Barth, A. I., Pollack, A. L., Altschuler, Y., Mostov, K. E., and Nelson, W. J. (1997) *J. Cell Biol.* **136,** 693–706
41. Nejsum, L. N., and Nelson, W. J. (2007) *J. Cell Biol.* **178,** 323–335
42. Bonifacino, J. S., and Traub, L. M. (2003) *Annu. Rev. Biochem.* **72,** 395–447
43. Deora, A. A., Gravotta, D., Kreitzer, G., Hu, J., Bok, D., and Rodriguez-Boulan, E. (2004) *Mol. Biol. Cell* **15,** 4148–4165
44. Schmidt, U., Briese, S., Leicht, K., Schürmann, A., Joost, H. G., and Al-Hasani, H. (2006) *J. Cell Sci.* **119,** 2321–2331
45. Hinners, I., Wendler, F., Fei, H., Thomas, L., Thomas, G., and Tooze, S. A. (2003) *EMBO Rep.* **4,** 1182–1189
46. Doray, B., Lee, I., Knisely, J., Bu, G., and Kornfeld, S. (2007) *Mol. Biol. Cell* **18,** 1887–1896
47. Gravotta, D., Deora, A., Perret, E., Oyanadel, C., Soza, A., Schreiner, R., Gonzalez, A., and Rodriguez-Boulan, E. (2007) *Proc. Natl. Acad. Sci. U.S.A.* **104,** 1564–1569
48. Fölsch, H., Ohno, H., Bonifacino, J. S., and Mellman, I. (1999) *Cell* **99,** 189–198
49. Toonen, R. F., de Vries, K. J., Zalm, R., Südhof, T. C., and Verhage, M. (2005) *J. Neurochem.* **93,** 1393–1400
50. Arunachalam, L., Han, L., Tassew, N. G., He, Y., Wang, L., Xie, L., Fujita, Y., Kwan, E., Davletov, B., Monnier, P. P., Gaisano, H. Y., and Sugita, S. (2008) *Mol. Biol. Cell* **19,** 722–734
51. Han, L., Jiang, T., Han, G. A., Malintan, N. T., Xie, L., Wang, L., Tse, F. W., Gaisano, H. Y., Collins, B. M., Meunier, F. A., and Sugita, S. (2009) *Mol. Biol. Cell* **20,** 4962–4975
52. Verhage, M., Maia, A. S., Plomp, J. J., Brussaard, A. B., Heeroma, J. H., Vermeer, H., Toonen, R. F., Hammer, R. E., van den Berg, T. K., Missler, M., Geuze, H. J., and Südhof, T. C. (2000) *Science* **287,** 864–869
53. He, B., and Guo, W. (2009) *Curr. Opin. Cell Biol.* **21,** 1–6
54. Sieber, J. J., Willig, K. I., Kutzner, C., Gerding-Reimers, C., Harke, B., Donnert, G., Rammner, B., Eggeling, C., Hell, S. W., Grubmüller, H., and Lang, T. (2007) *Science* **317,** 1072–1076
55. Lang, T., Bruns, D., Wenzel, D., Riedel, D., Holroyd, P., Thiele, C., and Jahn, R. (2001) *EMBO J.* **20,** 2202–2213
56. Li, C., Hao, M., Cao, Z., Ding, W., Graves-Deal, R., Hu, J., Piston, D. W., and Coffey, R. J. (2007) *Mol. Biol. Cell* **18,** 3081–3093